Enzyme Inhibitors

DOI: 10.1002/anie.200906696

Induced-Fit Binding of the Macrocyclic Noncovalent Inhibitor TMC435 to its HCV NS3/NS4A Protease Target

Maxwell D. Cummings, Jimmy Lindberg, Tse-I Lin, Herman de Kock, Oliver Lenz, Elisabet Lilja, Sara Felländer, Vera Baraznenok, Susanne Nyström, Magnus Nilsson, Lotta Vrang, Michael Edlund, Åsa Rosenquist, Bertil Samuelsson, Pierre Raboisson, and Kenneth Simmen*

The NS3 protein of hepatitis C virus (HCV), together with the NS4A peptide co-factor, comprises 685 residues and possesses domain-specific RNA helicase and serine protease activities.[1] NS3/NS4A protease activity is essential to the HCV life cycle.[2–4] Small-molecule inhibitors of NS3/NS4A protease have been widely explored[5–7] and are typically grouped into two classes: linear peptidomimetics with a ketoamide functionality that reacts with the catalytic Ser to form a reversible enzyme–inhibitor adduct, and noncovalent peptidomimetics containing a macrocycle[8] (e.g. Figure 1); macrocyclic ketoamide inhibitors have also been reported.[7] Macrocycles, underrepresented in synthetic drugs, are helpful in improving the druglike character of molecules.[9] TMC435 (**1**; Figure 1), a macrocyclic noncovalent inhibitor of NS3/NS4A protease with subnanomolar K_i values for genotype 1a and 1b NS3/NS4A proteases,[10,11] was discovered by optimizing an earlier NS3/NS4A protease inhibitor, BILN-2061 (**2**; Figure 1).[12] Key steps in the progression from **2** to **1** include reduction of macrocycle size, truncation of the P4[13] (P3 capping) group, conversion of the carboxylate "head group" to an acylsulfonamide, replacement of the P2 proline pyrrolidine with a cyclopentyl ring, and optimization of the substituted quinoline-thiazole ring system (Figure 1).[11,14–16] Despite exceeding three of four Lipinski[17] criteria,[18] **1** shows excellent pharmacokinetics in humans.[19]

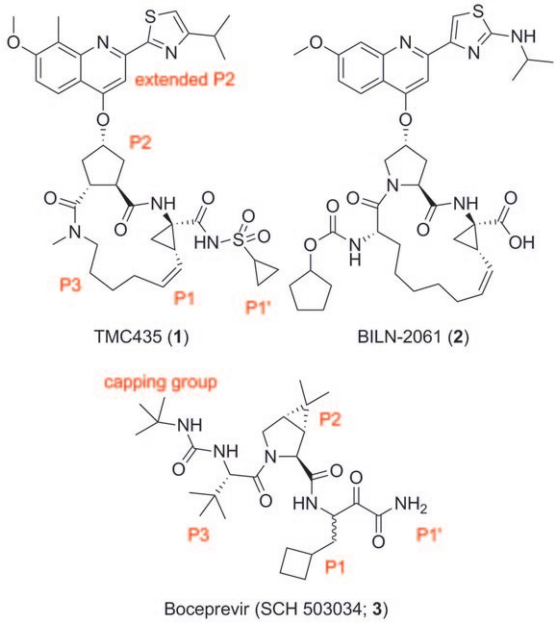

Figure 1. Macrocyclic (**1**, **2**) and ketoamide (**3**) inhibitors of HCV NS3/NS4A protease. Substrate positions[13] from NS3/NS4A protease complex structures are indicated for **1** and **3**.[39]

We have determined the crystal structure of **1** bound to its NS3/NS4A protease target from the BK strain of genotype 1b HCV at a resolution of 2.4 Å (Figure 2; see Table S1 and Figure S1 in the Supporting Information).[20] The three-dimensional structure of the NS3 protease domain in complex with a truncated version of the NS4A cofactor was first reported in 1996,[21] and that of an engineered single-chain NS3/NS4A protease–helicase construct in 1999.[1] Currently there are multiple covalent NS3/NS4A protease–inhibitor complexes accessible at the PDB. This structure is the first noncovalent NS3/NS4A protease–inhibitor complex to be deposited at the PDB. Additionally, the new structure shows that the large P2 substituent of **1** induces an extended S2 subsite to accommodate this group; none of the previously available complex structures share this feature.[22] We analyze the observed induced-fit binding of **1** to HCV NS3/NS4A protease, discuss key in vitro resistance mutations in the context of the complex, and disclose the new crystal structure for public analysis.

The structure of the NS3/NS4A–**1** complex shows the expected trypsin-like fold for the enzyme, with the inhibitor bound at the active site, spanning the S3–S1′ subsites (Figure 2; see Figure S1 in the Supporting Information). Unlike many other macrocyclic drugs that can be divided into functional (binding) and modulator (nonbinding) domains,[9] essentially all of **1** is involved in binding to its target site (Figure 2). Two canonical substrate-like intermolecular hydrogen bonds are observed: the P1–P2 backbone amide N contacts Arg155:O, and the carbonyl O of the P2–P3 amide

[*] M. D. Cummings, T.-I. Lin, H. de Kock, O. Lenz, P. Raboisson, K. Simmen
Tibotec BVBA
Gen De Wittelaan L 11B 3, 2800 Mechelen (Belgium)
Fax: (+32) 15-286-374
E-mail: mcummin1@its.jnj.com
J. Lindberg, E. Lilja, S. Felländer, V. Baraznenok, S. Nyström, M. Nilsson, L. Vrang, M. Edlund, Å. Rosenquist, B. Samuelsson
Medivir AB, Lunastigen 7, 14144 Huddinge (Sweden)

Supporting information for this article, including crystallography details, three additional figures and expanded references, is available on the WWW under http://dx.doi.org/10.1002/anie.200906696.

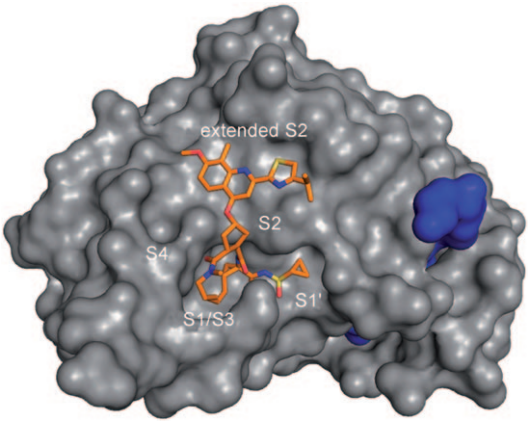

Figure 2. Crystal structure of the HCV NS3/4A protease-**1** complex (PDB ID 3KEE) at a resolution of 2.4 Å. Selected subsites in the active site of NS3/NS4A protease are indicated on the surface representation; NS3, gray; truncated NS4A peptide cofactor, blue; **1** color-by-atom, C orange, N blue, O red, S yellow.

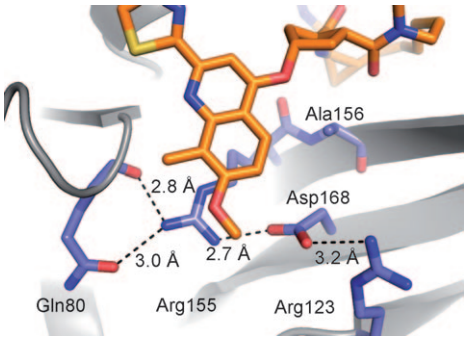

Figure 3. Details of the extended S2 subsite occupied by bound **1**.

contacts Ala157:N (see Figure S2 in the Supporting Information). In two of the four monomers in the asymmetric unit Lys136:NZ hydrogen bonds with the P1–P2 carbonyl O of **1** (see Figure S2 in the Supporting Information). The acylsulfonamide group of bound **1** forms an extensive network of intermolecular hydrogen bonds in the region of the catalytic Ser residue, effectively replacing the covalent interaction with the ketoamide warhead observed in other NS3/NS4A protease–inhibitor complexes. All four potential hydrogen-bonding partners of this inhibitor moiety form one or more intermolecular hydrogen bonds, involving Ser139:OG and His57:NE2 of the catalytic triad, and Gly137:N in the oxyanion hole (see Figure S2 in the Supporting Information). The cyclopropyl group of **1** occupies the S1′ subsite of the NS3/NS4A active site (Figure 2); Phe43 forms the base of this small but well-defined pocket (see Figures S2 and S3 in the Supporting Information). The extensive and complementary binding contacts of the acylsulfonamide and cyclopropyl substituents are consistent with the potency increase observed relative to terminal carboxylate analogues in this inhibitor series.[23] The P1- and P3-mimetic side chains of **1** are connected, forming a 14-membered macrocycle that also includes the P1–P3 backbone atoms of the peptidomimetic inhibitor (Figures 1 and 2; see Figure S2 in the Supporting Information). The S1/S3 subsite is a continuous and largely hydrophobic depression on the NS3/NS4A surface, and the inhibitor atoms that mimic substrate P1 and P3 side chains make hydrophobic binding contacts in this pocket with Val132, Leu135, Phe154, Ala157, Cys159 and the aliphatic part of Lys136 (Figure 2; see Figure S2 in the Supporting Information). The 14-membered macrocycle of **1** maintains the binding mode described previously for the 15-membered macrocycle of a **2**-like inhibitor.[24] Reduction of macrocycle size was an important goal during lead optimization, as we had previously observed that this improved human liver microsome stability, an important early pharmacokinetic marker.[25] The substituted phenyl group of the quinoline is positioned over the side chain of Arg155, while the pyridine-thiazole system is positioned over the catalytic residues His57 and Asp81. These groups, together with the cyclopentyl ring of bound **1**, shield this face of the catalytic region of the enzyme from bulk solvent (see also Ref. [26]).

Binding of **1** involves an induced-fit mechanism in an extended S2 subsite (Figure 3). With **1** bound, Arg155 adopts a conformation distinct from those observed in other structures available for analysis, including that of the full-length HCV helicase–protease,[1] the *apo* protease,[20,21,27] and various protease–inhibitor complexes (e.g. Figure 4). The S2 region of the NS3/4A protease active site has been studied extensively using experimental and computational approaches. Early circular dichroism studies with NS3/NS4A protease and product-based peptidic inhibitors indicated induced-fit binding.[28] Of specific relevance to the present work, a similar change was described for a chemical predecessor of **2**,[22,24] and we predicted the induced conformational change of Arg155 for binding of a close analogue of **1**.[14] Surface plasmon resonance studies with both **1** and **2** indicate a two-step binding mechanism consistent with an induced fit.[29] In the *apo* structure of full-length NS3/NS4A helicase–protease,[1] Arg155 projects toward the helicase domain and is stabilized by contacts with the Asp168 (protease domain) and Glu628 (helicase domain; Figure 4). A similar conformation is observed for Arg155 in NS3/NS4A

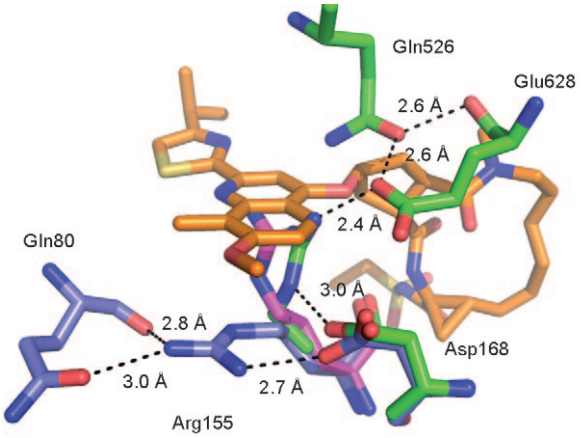

Figure 4. Different conformations in the extended S2 subsite region. Color-by-atom schemes: N blue, O red, S yellow; **1**, C orange; protein residues from **1** complex, C purple; **3** complex,[39] C magenta; *apo* NS3/NS4A protease–helicase,[1] C green; distances in Å.

protease complexes involving inhibitors with small P2 groups bound and in *apo* NS3/NS4A protease structures, although of course in these cases the stabilizing contacts with residues from the helicase domain are absent (e.g. Figure 4). This conformation precludes binding of **1**, and other inhibitors with large P2 groups, since the guanidine of Arg155 blocks the extended S2 region (Figure 4). In the induced conformation observed in the complex with **1**, the side chain of Arg155 adopts a distinctly different conformation, with stabilizing contacts involving Asp168, Gln80, and the quinoline of **1** (Figures 3 and 4). This change opens up the distal end of the commonly observed pocket, resulting in an extended S2 subsite that accomodates the large quinoline-thiazole P2 substituent of **1**. This observation encourages speculation on the role, if any, of the NS3 helicase domain in the binding of protease inhibitors, although a recent kinetic study showed minimal influence of the helicase domain on protease inhibitor activity.[30] It is clear, however, that conformational adaptability in the S2 region is essential for the inhibitory activity of **1** and other large P2 inhibitors, and that the S2 pocket for such inhibitors is near the observed protease–helicase interface.[1,24,31]

In vitro resistance profiling and subsequent site-directed mutation studies with HCV replicons identified mutations at residues Phe43, Gln80, Arg155, Ala156, and Asp168 that reduced the inhibition of HCV replication by **1** to varying degrees.[32] Interestingly, all of these residues have been noted previously in the context of in vitro resistance selections and/or natural sequence variation,[33–35] and most have been observed during clinical trials with **1** or other NS3/NS4A protease inhibitors.[19,36,37] These observations can be rationalized based on the structure of the NS3/NS4A protease–**1** complex. As noted above, Gln80, Arg155, and Asp168 form part of the extended S2 subsite induced by binding of **1** (Figure 3; see Figure S2 in the Supporting Information). Most significantly, mutant replicon studies show that changes to Asp168 yield reductions in the effect of **1** ranging from 5- to 2000-fold, dependent upon the specific mutation.[32] The **1**-induced conformation of R155 is stabilized by interactions with Gln80 and Asp168. Modeling studies conducted by ourselves (not shown, but see Figures 3 and 4) and others[33,38] suggest that mutation of Asp168 destabilizes the subsite conformation required for inhibitor binding, and also indicate that certain mutations of Asp168 sterically preclude the Arg155 conformation required for binding of **1**. Thus, the observed mutation effects for Asp168 are consistent with the intricate network of stabilizing interactions observed in the extended S2 subsite (Figure 3). Ala156 is positioned on the edge of the proximal region of S2 near the backbone of bound **1**, and makes several close contacts with the bound inhibitor (Figure 3; see Figures S2 and S3 in the Supporting Information). Consistent with this central position, Ala156 has been identified in in vitro resistance studies with NS3/NS4A protease inhibitors of various chemotypes.[36] Phe43 forms the base of the S1′ pocket, and changes at this position can impact binding of the cyclopropyl P1′ moiety (see Figures S2 and S3 in the Supporting Information). Furthermore, adjustments in the binding mode resulting from changes in this subsite could disturb the complex network of intermolecular hydrogen bonds involving the adjacent acylsulfonamide group and the catalytic Ser nucleophile (see Figure S2 in the Supporting Information).

Overlay of the NS3/NS4A protease complexes of **1** and **3**[39] highlights the relationship between the macrocycle and large P2 group of **1** and the corresponding groups of **3** (Figures 1 and 5). For the macrocycle of **1**, rigidification is achieved while maintaining occupancy of the S1/S3 subsite with atom types similar to those of **3** (Figure 5). Canonical

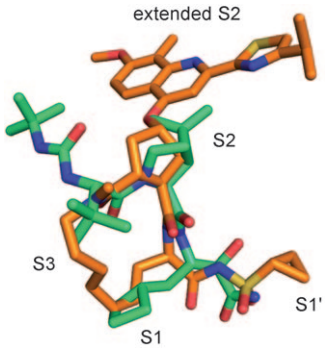

Figure 5. Overlay of bound **1** and **3**.[39] Corresponding subsite regions of the NS3/NS4A protease active site occupied by **1** are indicated; N blue, O red, S yellow; **1**, C orange; **3**, C green.

intermolecular enzyme–substrate-like hydrogen bonds beyond that of the P3 carbonyl are not possible for **1**, since it is essentially truncated in the middle of P3, with C_α converted to a dialkylated amide N and one of the N-alkyl groups mimicking the macrocyclized P3 side chain. This is distinct from other NS3/NS4A protease inhibitors, which typically extend well beyond P3 (e.g. Figures 1 and 5). The noncovalent acylsulfonamide overlays with the covalent ketoamide serine trap. In the optimization effort that yielded **1**, replacement of the original carboxylate "head group" by the acylsulfonamide moiety improved NS3/NS4A affinity and cell-based activity.[23] N-terminal truncation partially compensates for the polar surface area increase due to this change, and further reduces the peptidic nature of the molecule; N-terminal truncation of a close structural analogue of **1** significantly improved human liver microsome stability.[15] Consequently, **1** has an excellent pharmacokinetic profile in humans,[19] and is currently being evaluated as a once-daily anti-HCV agent.

As discussed above, NS3/NS4A protease inhibitors are typically denoted as either (noncovalent) macrocycles or linear ketoamides. The additional distinction of large versus small P2 groups is not readily apparent with this classification scheme. Inhibitor size difference at this position seems noteworthy (e.g. Figure 5), given the requirement for an induced fit to accommodate binding of the large P2 moieties (Figure 4) and the proximity of the extended subsite to the protease-helicase interface (Figure 4).

In summary, we have determined the crystal structure of the macrocyclic inhibitor TMC435 bound to its HCV NS3/4A protease target at a resolution of 2.4 Å, providing atomic detail of induced fit to an extended S2 subsite. The complex

structure helps to rationalize the impact of key modifications in the optimization path that led to **1**, and is guiding our understanding of resistance patterns. Future modeling and structure-based design efforts aimed at NS3/NS4A protease should benefit from the new structure, which represents the first example of a noncovalent NS3/NS4A protease–inhibitor complex deposited in the PDB and details the induced fit involved in accommodating a large P2 substituent. Inhibitors with large P2 groups that occupy the extended S2 subsite probe the crystallographically observed helicase-protease interface, and it is hoped that future studies will clarify the relevance of interfacial contacts to protease activity and protease inhibitor binding.

Received: November 27, 2009

Keywords: drug design · hepatitis C · inhibitors · protein structures

[1] N. Yao, P. Reichert, S. S. Taremi, W. W. Prosise, P. C. Weber, *Structure* **1999**, *7*, 1353.
[2] R. Bartenschlager, L. Ahlborn-Laake, J. Mous, H. Jacobsen, *J. Virol.* **1993**, *67*, 3835.
[3] A. Grakoui, D. W. McCourt, C. Wychowski, S. M. Feinstone, C. M. Rice, *J. Virol.* **1993**, *67*, 2832.
[4] L. Tomei, C. Failla, E. Santolini, R. De Francesco, N. La Monica, *J. Virol.* **1993**, *67*, 4017.
[5] S. H. Chen, S. L. Tan, *Curr. Med. Chem.* **2005**, *12*, 2317.
[6] J. A. Thomson, R. B. Perni, *Curr. Opin. Drug Discov. Devel.* **2006**, *9*, 606.
[7] S. Venkatraman, F. G. Njoroge, *Expert Opin. Ther. Pat.* **2009**, *19*(9), 1277–1303.
[8] A ring with $\geq$12 member atoms.
[9] E. M. Driggers, S. P. Hale, J. Lee, N. K. Terrett, *Nat. Rev. Drug Discovery* **2008**, *7*, 608.
[10] T. I. Lin et al., *Antimicrob. Agents Chemother.* **2009**, *53*, 1377.
[11] P. Raboisson et al., *Bioorg. Med. Chem. Lett.* **2008**, *18*, 4853.
[12] Y. S. Tsantrizos, *Biopolymers* **2004**, *76*, 309.
[13] I. Schechter, A. Berger, *Biochem. Biophys. Res. Commun.* **1967**, *27*, 157.
[14] M. Bäck et al., *Bioorg. Med. Chem.* **2007**, *15*, 7184.
[15] P. Raboisson et al., *Bioorg. Med. Chem. Lett.* **2008**, *18*, 5095.
[16] S. Vendeville et al., *Bioorg. Med. Chem. Lett.* **2008**, *18*, 6189.
[17] C. A. Lipinski, F. Lombardo, B. W. Dominy, P. J. Feeney, *Adv. Drug Delivery Rev.* **1997**, *23*, 3.
[18] MW = 750, #HD = 2, #HA = 12, ClogP = 5.3.
[19] H. W. Reesink et al., *Gastroenterology*, in press.
[20] We also report a 2.5 Å resolution apo structure of H strain genotype 1a NS3/4A protease (PDB ID 3KF2), similar to that described previously in conjunction with the NS3/4A protease complex of 3.[39]
[21] J. L. Kim et al., *Cell* **1996**, *87*, 343.
[22] This type of structural adaptation was described previously for an analog of 2.[24] However, a detailed analysis of the altered interactions was not reported, and the reported crystal structure has not been made available for public analysis.
[23] Tables 1 and 2 of [14] present acid/sulfonamide analogue pairs for which the difference in K_i is as high as 440-fold (eg. 31 nM/0.07 nM, respectively).
[24] Y. S. Tsantrizos, G. Bolger, P. Bonneau, D. R. Cameron, N. Goudreau, G. Kukolj, S. R. LaPlante, M. Llinas-Brunet, H. Nar, D. Lamarre, *Angew. Chem.* **2003**, *115*, 1394; *Angew. Chem. Int. Ed.* **2003**, *42*, 1356.
[25] This trend is clearly shown in Table 1 of [15].
[26] N. Goudreau, D. R. Cameron, P. Bonneau, V. Gorys, C. Plouffe, M. Poirier, D. Lamarre, M. Llinas-Brunet, *J. Med. Chem.* **2004**, *47*, 123.
[27] R. A. Love, H. E. Parge, J. A. Wickersham, Z. Hostomsky, N. Habuka, E. W. Moomaw, T. Adachi, Z. Hostomska, *Cell* **1996**, *87*, 331.
[28] E. Bianchi, S. Orru, F. Dal Piaz, R. Ingenito, A. Casbarra, G. Biasiol, U. Koch, P. Pucci, A. Pessi, *Biochemistry* **1999**, *38*, 13844.
[29] T.-I. Lin, B. Devogelaere, unpublished results.
[30] D. Thibeault, M. J. Massariol, S. Zhao, E. Welchner, N. Goudreau, R. Gingras, M. Llinas-Brunet, P. W. White, *Biochemistry* **2009**, *48*, 744.
[31] N. J. Liverton et al., *J. Am. Chem. Soc.* **2008**, *130*, 4607.
[32] The in vitro resistance profile of TMC435 is discussed in detail in O. Lenz et al., submitted.
[33] X. Tong et al., *Biochemistry* **2006**, *45*, 1353.
[34] X. Tong et al., *Antiviral Res.* **2008**, *77*, 177.
[35] F. X. Lopez-Labrador, A. Moya, F. Gonzalez-Candelas, *Antiviral Ther.* **2008**, *13*, 481.
[36] G. Koev, W. Kati, *Expert Opin. Invest. Drugs* **2008**, *17*, 303.
[37] T. L. Kieffer, A. D. Kwong, G. R. Picchio, *J. Antimicrob. Chemother.* **2010**, *65*(2), 202–212.
[38] C. Lin et al., *J. Biol. Chem.* **2004**, *279*, 17508.
[39] A. J. Prongay et al., *J. Med. Chem.* **2007**, *50*, 2310.

